Lithos 112 (2009) 277–288

Contents lists available at ScienceDirect

Lithos

journal homepage: www.elsevier.com/locate/lithos

Reequilibration of fluid inclusions: Bulk-diffusion

Ronald J. Bakker *

Department of Applied Geosciences and Geophysics, Mineralogy and Petrology Group, University of Leoben, Peter-Tunner-Strasse 5, A-8700 Leoben, Austria

ARTICLE INFO

Article history:
Received 15 August 2008
Accepted 9 March 2009
Available online 19 March 2009

Keywords:
Diffusion
Quartz
Fluid inclusions
Re-equilibration

ABSTRACT

Bulk diffusion of fluid components through quartz, which is a nominally anhydrous mineral, is one of a series of processes that may alter fluid inclusions in crystals. Diffusion of water through quartz has been considered an important factor for re-equilibration of fluid inclusions. However, the solubility of water in quartz, the nature of the diffusing water-related molecules, and diffusion coefficients have not been adequately determined to calculate reliable rates of inclusion alteration. A new three-dimensional mathematical diffusion model is presented to characterize bulk diffusion in quartz with randomly distributed fluid inclusions. This model assumes an infinite external fluid source and treats fluid inclusions as instantaneous point sources. The computer program "ReqDif" from the software package "FLUIDS" (http://fluids.unileoben.ac.at) can be used to calculate the effect of diffusion with self-defined parameters. Using a diffusion coefficient of 10^{-12} m^2 s^{-1} (±60%), the rate of H_2O loss or gain of most inclusions is relatively high, adapting them within several 10,000 of years to new pore fluid conditions. However, diffusion according to this model may be restricted and partly inhibited by several important factors, such as the low porosity in metamorphic rock and relative low temperatures in sedimentary and diagenetic rocks. The imprecision of estimated diffusion coefficients, and the undetermined accuracy do not allow reliable diffusion calculations. Diffusion along micro-cracks and dislocations is a more efficient process to transport fluid components through quartz.

1. Introduction

Constant fluid density and composition are the main prerequisites for the use of fluid inclusions as important relicts and indicators of processes and conditions of entrapment during the geological history of the rock. In metamorphic rock, fluid inclusions with highly variable contents (i.e. fluid composition and density) may coexist. Disregarding any interpretation of the processes responsible for the formation of fluid inclusion assemblages of variable water-content, it remains an undisputed observation that such assemblages have persisted over geological time, despite any post-entrapment changes, that may have altered individual inclusions differently (e.g. Touret, 2001).

Diffusion of fluid components through quartz (among other minerals) is a process that may change the properties of fluid inclusions. In theory, both density and composition may change as a result of transport of fluid components through the quartz crystal. Quartz is a nominally anhydrous mineral that may contain maximally 40 μg H_2O per gram SiO_2 (e.g. Kronenberg, 1994), whereas the presence of microscopic fluid inclusions may result in a total water content up to several thousands μg per gram SiO_2 (see review of Johnson, 2006, and reference therein). Due to the variation in concentration of water in single quartz grains, water is able to diffuse through H_2O-undersaturated quartz crystals. Unfortunately, relatively little is known about diffusion of fluid components through quartz (see also Ingrin and Blanchard, 2006). The aim of this study is to scrutinize the available experimental work, which have been accomplished to study solubility and diffusion in quartz. A new mathematical model according to Fick's laws of diffusion is developed to be able to predict bulk-diffusion in quartz, with specific diffusion coefficients, between pore fluids and fluid inclusions, in order to be able to characterize their alteration as a function of temperature and pressure conditions and specific chemical potentials of corresponding fluid components.

2. Principles of water diffusion in quartz

The concentration of H_2O in quartz and diffusion of H_2O through quartz cannot be measured directly. Theoretically, water-related species can be present in a variety of components within the quartz crystal, such as molecular H_2O, ionic OH^-, H^+, O^{-2}, and gaseous O_2 and H_2. Efficient diffusion modelling can only be performed if the diffusing fluid component is well defined by its chemical composition and its position in the quartz lattice. The presence of water-related species in quartz was illustrated with infrared absorption spectroscopy for hydroxyl groups and H_2O related species (e.g. Paterson, 1982; Kronenberg, 1994; Libowitzky and Rossman, 1997; Bachheimer, 2000), and with ion microprobe analysis using secondary ion mass spectroscopy which analyses the isotopic composition of oxygen in quartz (e.g. Giletti and Yund, 1984; Dennis, 1984), that was coupled to hydrogen in diffusing heavy water ($H_2^{18}O$). Infrared spectroscopy can distinguish between hydrogen present as OH^- groups (hydroxyl) and

* Tel.: +43 3842 4026201; fax: +43 3842 47016.
E-mail address: ronald.bakker@mu-leoben.at.

0024-4937/$ – see front matter © 2009 Elsevier B.V. All rights reserved.
doi:10.1016/j.lithos.2009.03.006

molecular H_2O (Aines et al., 1984), but it cannot specify the presence of hydrogen (OH^-) as an interstitial- or substitutional-impurity species. Moreover, molecular H_2O can be present in either small fluid inclusion or as interstitial impurities.

Transport of fluid components occurs along concentration gradients in a homogeneous medium (e.g. a quartz crystal). In other words, the chemical potential gradient of H_2O, or gradient in H_2O fugacity inside the quartz is a driving force for water diffusion in or out fluid inclusions. The variety of initial and boundary conditions in diffusion experiments, such as the initial distribution of the diffusing species, results in a variety of mathematical equations to describe diffusion according to Fick's law (e.g. Crank, 1979; Brady, 1995). Experimentally, concentration profiles provide the fundamental contributions for the selected diffusion model. The major physical assumption of diffusion processes according to these equations is the ability of molecules to move randomly. Diffusion coefficients (D in $m^2\ s^{-1}$) are determined from the mathematical analyses of concentration profiles of specific fluid components in quartz. Its variation with temperature is expressed in an Arrhenius plot (Eq. (1))

$$D_i(T) = D_i^0 \exp\left(\frac{-\Delta H_i}{RT}\right) \quad (1)$$

where i is the diffusing fluid component, D_i^0 is a diffusion constant specific for quartz and the fluid component i, and ΔH_i is the activation energy (in J mol^{-1}) or enthalpy, R is the gas constant ($=8.31451$ J mol^{-1} K^{-1}) and T is temperature (in K).

3. Solubility of water in quartz

Water can be present in quartz in three specific manners (e.g. Aines et al., 1984; Kronenberg, 1994; Catlow et al., 1995), also known as extrinsic point defects: 1. as interstitial impurities (positioned between regular Si and O lattice sites); 2. as substitutional impurities (replacing Si or O in the crystal lattice); and 3. as fluid inclusions (variable sizes between nm and several μm's). Absorbed water is not taken into account in the present study, because it occurs at the surface of quartz and not within the crystal. Therefore, silanol groups that may also form in dislocations are not considered (e.g. Griggs, 1967).

The interstitial impurities can occur in the form of neutral H_2O molecules or as H^+ ions, which may compensate Fe^{3+} and Al^{3+} substitutes at Si^{4+} lattice positions. The hydrogen concentration is in the order of several 10 to 100 μmol H per mole Si (e.g. Kronenberg et al., 1986), and corresponds to the Al^{3+} and Fe^{3+} impurities concentration in quartz. Therefore, the Al and Fe concentration is a measure for the maximum possible uptake of hydrogen in quartz. An increase of the crystal defect concentration (i.e. the Al and Fe impurities) at higher pressures may result in an increase of hydrogen solubility, similar to experimental observations in olivine and garnets (e.g. Demouchy et al., 2005). Experimental deformation studies illustrate that the solubility of molecular H_2O in natural quartz cannot be estimated within the limits of the experimental setups (e.g. Kronenberg et al., 1986; Gerretsen et al., 1989). In other words, molecular H_2O did not significantly diffuse in to "dry" natural quartz, and it is supposed to be controlled by the relatively slow oxygen transport. Therefore, the solubility of molecular H_2O as interstitial impurity is unknown, and cannot be modelled according to substitutes (c.f. Paterson, 1986) as it diffuses and remains in a molecular state within the quartz crystal. In theory, it is expected that the solubility of interstitial impurities decrease with increasing pressure, as the available space in the crystal lattice, i.e. a decrease in the Si–O bond length, will become smaller by pressure-induced contraction. A solubility decreases with increasing pressure at constant temperature and water fugacity has also been observed in silicate melts (e.g. Stolper, 1982).

Substitution may consist in replacing one Si^{4+} ion with four H^+ ions, i.e. the $(4H)_{Si}$ defect (also known as "hydrogarnet" defects), which corresponds theoretically to the molecular oxides substitution of one SiO_2 with two H_2O molecules. The equilibrium solubility of this impurity in synthetic quartz has been thermodynamically modelled by Paterson (1986), Doukhan and Paterson (1986), and Rosa et al. (2005), and does not exceed about 100 μmole H per mole Si (c.f. Kronenberg et al., 1986). These models predict an increase of impurity-solubility with pressure, as observed in the β-quartz stability field.

Fluid inclusions are the only "visible" containers in quartz crystals (optically and electron-microscopically) that may contain variable amounts of H_2O. Small "bubbles" observed with electron microscopy (TEM) in annealed synthetic quartz (e.g. McLaren et al., 1983; Cordier et al., 1988) are regarded as small fluid inclusions that contain molecular water. They may be responsible for the relatively high estimated hydrogen content in some quartz (up to 3000 μmol H per mole Si, see also Kronenberg, 1994). The small inclusions are nanometer-sized including only several thousands of water molecules, in which ice-nucleation is extremely inhibited (the detection of ice in quartz at low temperatures implies the presence of molecular H_2O). This metastability is also observed during microthermometrical measurements of micrometer-sized fluid inclusions (see also Shepherd et al., 1985), which illustrates the nucleation problems of freezing H_2O in micropores (e.g. Angell et al., 1973, Bakker, 2004).

In conclusion, the solubility of H_2O in quartz involves a series of water-related species, which are present as impurities or fluid inclusions. The solubility of individual species is unknown or highly variable, but the number of interstitial impurities is related to cation impurities in quartz (Al and Fe). The variation of solubility with temperature, pressure and an external H_2O fugacity is unknown. It is most likely that the major part of H_2O in quartz is present as fluid inclusions. In the present study, the solubility of only extrinsic impurities (see Appendix A) is taken into account (i.e. the sum of interstitial and substitutional impurities), which are considered to represent the most efficient species that diffuse through quartz.

4. Diffusion of water through quartz

4.1. Bulk- and pipe-diffusion

Deformation experiments have revealed the existence of "hydrolytic weakening" in quartz (e.g. Griggs and Blacic, 1965; Griggs, 1974). The processes considered to be involved in "hydrolytic weakening" also include the mobility of water through quartz crystals. However, diffusion of molecular H_2O in natural quartz is too slow within the limits of experimentation to provide "hydrolytic weakening" (Kronenberg et al., 1986; Gerretsen et al., 1989). The experimentally estimated bulk-diffusion coefficients of H_2O were not efficient enough to distribute water in the observed volume of deformed quartz. Therefore, diffusion of water through dislocations (i.e. pipe- or core-diffusion) was already considered by Griggs (1974) to explain the hydrolytic weakening of quartz. Alternatively, the observed strain after deformation experiments in natural quartz crystals was suggested to result from microcracking and crack-assistant diffusion of H_2O (Kronenberg et al., 1986; Gerretsen et al., 1989).

The mobility of hydrogen through quartz was indirectly experimentally proven by its presence and reactivity in fluid inclusions (Mavrogenes and Bodnar, 1994), by formation of water inclusion in synthetic quartz (McLaren et al., 1983; Cordier et al., 1988), and by increased water solubility in natural quartz as obtained from infrared spectroscopy (Kronenberg et al., 1986). The latter two studies involve diffusion of molecular H_2O through quartz. The growth of water inclusions in annealing experiments of synthetic quartz was assumed to proceed by Si and O diffusion along dislocations (McLaren et al., 1983), whereas Cordier et al. (1988) suggested rapid exchange of water and quartz along the same dislocations to increase the size of individual bubbles and reduce the amount. The mobility of H_2O along dislocations was also proposed by Bakker and Jansen (1990) and Heggie (1992).

Pipe-diffusion coefficients are unknown, but are considered to have substantial higher values than bulk-diffusion coefficients.

In the present study, transport of water through quartz according to bulk-diffusion is considered, and diffusion is isotropic. It must be noted that the presence of line defects (e.g. dislocations) or crystallographically defined channels may enhance diffusion in specific directions, i.e. anisotropic diffusion.

4.2. Experimental diffusion coefficients of fluids in quartz

The generally applied experimental method to determine diffusion coefficients of H_2O, O_2 and CO_2 is a bulk exchange technique based on the exchange reaction of isotopes between fluid and mineral (see also Freer and Dennis, 1982). The measured concentration profiles are the result of at least two processes (see also Giletti, 1986), i.e. diffusion of a component in the mineral and the exchange reaction of isotopes. The estimated "diffusion coefficients" from these experiments may only reflect isotope reactivity, if the exchange reaction in the mineral lattice is the rate limiting step. Oxygen is most favourable for diffusion experiments, because it is a major component of both minerals and fluids, and its isotopes are relatively easily available for experimental studies. In addition, isotopic concentrations in minerals are relatively easily obtained from ion microprobe analyses (e.g. Giletti et al., 1978; Sharp et al., 1991). A self-diffusion coefficient was estimated for ^{18}O (Dennis, 1984; Giletti and Yund, 1984; Elphick et al., 1986; Sharp et al., 1991; Farver and Yund, 1991), and a tracer diffusion coefficient (i.e. chemical diffusion coefficient) was estimated for Deuterium (e.g. Kronenberg et al., 1986).

Most diffusion experiments were performed under hydrothermal conditions in the β-quartz stability field, with water as an external infinite medium with a fixed isotope concentration, i.e. water was doped with either $H_2^{18}O$ or D_2O. The nature of the diffusing component is an uncertainty in most experimental studies on oxygen diffusion in minerals. The presence of water enhances oxygen diffusion in quartz (e.g. Farver and Yund, 1991), therefore, it is assumed that H_2O is the major diffusing particle that transports oxygen through the quartz crystal. Anhydrous experiments with doped carbon dioxide ($C^{18}O_2$) (Sharp et al., 1991) and "dry" oxygen (Haul and Dümbgen, 1962) reveal a 100 to 10^6 times slower diffusion of oxygen, respectively, than hydrothermal experiments. A direct relationship between experimentally determined diffusion coefficients for fluid components such as H_2O, O_2 and CO_2 and pore fluid concentrations was not established.

4.3. Mathematical solution of Fick's laws

A mathematical diffusion model is based on solving Fick's first and second law of isotropic diffusion (see also Crank, 1979; Carslaw and Jaeger, 1986). Mathematically modelling of fluid components through quartz is generally based on one-dimensional diffusion (e.g., Brady, 1995) in a semi-infinite body with a constant surface concentration (Eq. (2)).

$$c_i^{qtz}(x,t) = \frac{1}{2}\left(c_i^{max} - c_i^0\right)\cdot erfc\left(\frac{x}{2\sqrt{D_i t}}\right) + c_i^0 \quad (2)$$

where x is the distance from the surface in the crystal, t is time (in s), c is the concentration in quartz (in mol i per litre SiO_2), and the superscripts max and 0 reflect the maximum solubility in quartz at a given temperature and pressure, and the starting concentration, respectively. The uncertainty in the estimated diffusion coefficients for oxygen in quartz is about 40% (Freer and Dennis, 1982). Most experimental results are in agreement with this mathematical formulation close to the grain boundary, but are deviating at greater depths (e.g. Freer and Dennis, 1982; Dennis, 1984). The experimental setup of those studies does not exclude three-dimensional diffusion through the quartz crystal. Consequently, much lower diffusion coefficients can be estimated for similar concentration profiles than in one-dimensional diffusion models.

4.4. Case study: re-evaluation of experimental data from Kronenberg et al. (1986)

The accuracy and reliability of reported diffusion coefficients of water-related species through quartz are tested with the experimental data from Kronenberg et al. (1986). Their analytical method includes the estimation of hydrogen concentration in cylindrical quartz cores of 6.3 mm diameter and approximately 3.26 mm in length with IR spectroscopy. The starting material (crystal A-1 in Kronenberg et al., 1986) has a concentration of 34 μmol H per mol Si. The maximum measured concentration in quartz is about 97 μmol H per mol Si, which is assumed to represent the maximum concentration at all p–T conditions. The uncertainty in all concentration measurements is approximately 10 μmol per mol.

Kronenberg et al. (1986) have selected a one-dimensional diffusion model in a finite-sheet with a fixed surface concentration that was simplified for relative short time intervals (c.f. Eq. 4.19 in Crank, 1979). The general mathematical solution for this diffusion model at any time is given by Eq. (3) (c.f. Eq. 4.17 in Crank, 1979).

$$c_H^{qtz} = \left(c_H^{max} - c_H^0\right) \times\left[1 - \frac{4}{\pi}\sum_{n=0}^{\infty}\frac{(-1)^n}{2n+1}\exp\left(\frac{-(2n+1)^2\pi^2 Dt}{4L^2}\right)\cdot\cos\left(\frac{(2n+1)\pi x}{2L}\right)\right] + c_H^0 \quad (3)$$

where c_H^{max} is the maximum concentration of H in β-quartz at given temperature and pressure conditions, c_H^0 is the starting concentration before experimentation, L is half the thickness of the sheet (in m), D is the diffusion constant (in $m^2\ s^{-1}$), t is time (in s) and x is one-dimensional distance from the centre of the sheet (in m). Diffusion was assumed to take place only in the direction perpendicular to the top and bottom of a cylinder. Therefore, the surface of the sheet in Eq. (3) is limited to only 31 mm^2 ($=\pi r^2$), and $2\cdot L$ is the length of the cylinder.

Eq. (3) has been used in this study to recalculate D values for a part of the data given by Kronenberg et al. (1986, their Table 2). At 800 °C and a constant water pressure of 890 MPa (see Table 1a), the newly calculated diffusion coefficients vary systematically with time (Fig. 1), which indicates that the selected diffusion model is incorrect. Furthermore, the uncertainties are about 60%, which indicates the difficulty with which those numbers are obtained. The diffusion coefficient given by Kronenberg et al. (1986) corresponds accidentally to the average value obtained from Table 1a, i.e. $(23\pm14)\cdot10^{-12}\ m^2\ s^{-1}$. The scarce data at 700 and 900 °C (Tables 1b and 2, respectively) do not allow determination of correlations with partial water pressure or temperature. The calculated diffusion coefficients at these temperatures are similar and not substantial different from those obtained at 800 °C (see Fig. 1). All recalculated diffusion coefficients illustrate the previously

Table 1a
Diffusion coefficients for hydrogen in β-quartz, at 800 °C and 890 MPa water pressure (from Brucite buffer), as calculated from the concentration in the center of the sample (data from Kronenberg et al., 1986).

Exp. Nr	Fluid source	Exp. time s	μmol H per mol Si	D $m^2\ s^{-1}$
N-563	H_2O (// c)	$9.18\cdot10^3$	42 ± 10	$(51\pm40)\cdot10^{-12}$
N-579	H_2O (⊥ c)	$1.45\cdot10^4$	56 ± 10	$(47\pm34)\cdot10^{-12}$
N-569	H_2O (// c)	$2.21\cdot10^4$	69 ± 10	$(49\pm27)\cdot10^{-12}$
N-561	H_2O (// c)	$1.74\cdot10^5$	91 ± 10	$(17\pm11)\cdot10^{-12}$
N-556	H_2O (// c)	$1.77\cdot10^5$	72 ± 10	$(7.2\pm3.9)\cdot10^{-12}$
N-562	H_2O (// c)	$1.90\cdot10^5$	82 ± 10	$(11\pm6)\cdot10^{-12}$
N-581	H_2O (// c)	$6.04\cdot10^5$	80 ± 10	$(3.1\pm1.8)\cdot10^{-12}$

Thickness of cylinder is 3.26 mm (L), diameter is 6.3 mm (see also Fig. 2b). The starting concentration c_0 is rounded to 35 ± 10 μmol H per mol Si, and c_{max} is rounded to 100 ± 10 μmol H per mol Si.

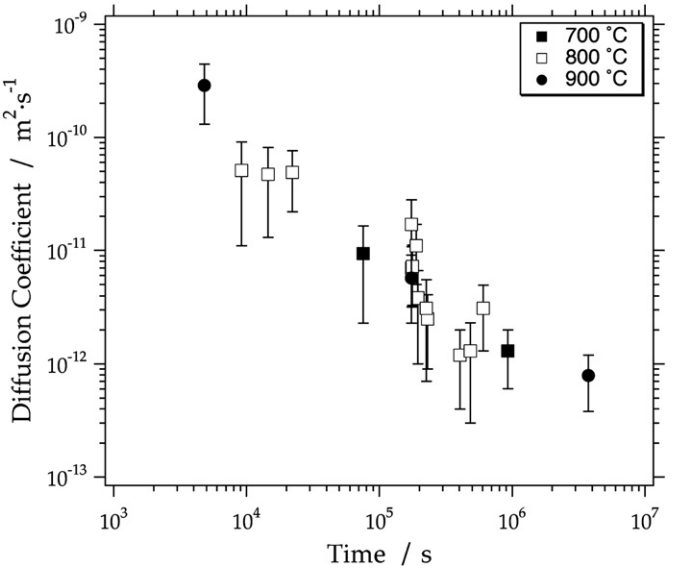

Fig. 1. Recalculated diffusion coefficients of water through quartz at variable diffusion times and temperatures according to experimental data from Kronenberg et al. (1986).

described dependence with experimentation time (Fig. 1). The results of this re-evaluation are in contrast with the interpretations from Kronenberg et al. (1986), that also include an unmistakable temperature dependence.

The variation of diffusion coefficients with the partial H_2O pressure at 800 °C is given in Table 3. Despite the large uncertainties, a trend of increasing D values at higher water pressures, from 1100 to 1600 MPa, is illustrated in Fig. 2. Including the data at lower H_2O pressures from Table 1a, a reversed trend is observed in the pressure range of 800 to 1100 MPa. These trends are not necessary in contradiction as they may represent two different processes that dominated in different pressure domains, i.e. a decrease in ultimate solubility with increasing pressure, and an increase in diffusion as more H_2O is available in the external source (see also paragraph 3).

In conclusion, the data of Kronenberg et al. (1986) do not allow the estimation of temperature dependence of diffusion coefficients and, therefore, the Arrhenius equation cannot be used to obtain D_i^0 values and activation energies (see Eq. (1)). A correct diffusion model should include three-dimensional diffusion, which results in the estimations of lower D values for the same concentration profiles. Consequently, the diffusion coefficients obtained from one-dimensional models (Eq. (3)) for relatively low times ($t<10^5$ s) overestimate correct values, whereas at high times ($t>10^5$ s) the coefficients approach accurate values. The diffusion coefficient of water through β-quartz calculated with these data is approximately 10^{-12} m^2 s^{-1} at temperatures between 700 and 900 °C, which corresponds to the lowest values in Figs. 1 and 2. It must be noted that the uncertainty in this value is about 60%.

5. Diffusion model for quartz containing fluid inclusions

Qin et al. (1992) presented a diffusion model for a perfect spherical quartz crystal with exactly in the centre a spherical inclusion, either melt or fluid, in order to study re-equilibration behaviour of inclusions (see Appendix B). In the present study, some of the starting conditions and assumptions have been changed, including the boundary conditions and mathematical approach to model diffusion with randomly distributed fluid inclusions in a spherical quartz crystal.

Table 1b
Diffusion coefficients for hydrogen in β-quartz at 700 °C and variable water pressures.

Exp Nr.	p(H_2O) MPa	Fluid source	time s	μmol H per mol Si	D m^2 s^{-1}
N-557	400	H_2O (// c), brucite buffer	$9.27 \cdot 10^5$	71 ± 10	$(1.3 \pm 0.7) \cdot 10^{-12}$
N-597	1540	H_2O (// c), water	$7.57 \cdot 10^4$	54 ± 10	$(9.4 \pm 7.1) \cdot 10^{-12}$

Table 2
Diffusion coefficients for hydrogen in β-quartz at 900 °C and variable water pressures, re-interpreted data from Kronenberg et al. (1986).

Exp Nr.	p(H_2O) MPa	Fluid Source	time s	μmol H per mol Si	D m^2 s^{-1}
N-613	1550	H_2O (// c), water	$3.75 \cdot 10^6$	98 ± 10	$(0.79 \pm 0.41) \cdot 10^{-12}$
N-595	1510	H_2O (// c), water	$4.80 \cdot 10^3$	74 ± 10	$(289 \pm 158) \cdot 10^{-12}$
N-578	1420	H_2O (// c), brucite buffer	$1.74 \cdot 10^5$	66 ± 10	$(5.7 \pm 3.4) \cdot 10^{-12}$

5.1. Starting conditions

A spherical quartz grain with radius b is considered in a three-dimensional diffusion model (Fig. 3). This grain contains a spherical fluid inclusion with radius a, which is not in the centre. In general, the size difference between grain and inclusion is a multiplication factor 1000 to 10,000. For example, a grain may have a diameter of 5 mm, whereas generally the inclusion may have a diameter of 0.5 to 5 μm. The reference of the coordination system for quartz around the spherical fluid inclusion is the inclusion centre (radial distance r_f), and, therefore, differently from the quartz grain (radial distance r_q) (see Fig. 3). The quartz crystal is floating freely in a fluid (infinite source), i.e. the total quartz surface is in contact with a pore fluid that may diffuse into the grain.

As a result of the diffusion process, the concentration of H_2O in the quartz grain is a function of distance to the centre of the grain (r_q) and time (t), and varies until equilibrium is reached. It should be noted that diffusion between a pore fluid and fluid inclusions will not be effective in a saturated quartz crystal. The fugacity of water in the fluid inclusion and in the pore fluid is obtained from an equation of state for fluid mixtures, e.g. a unified Helmholtz energy function for pure water according to Haar et al. (1984), or a modified Redlich–Kwong equation of state for H_2O–CO_2 mixture according to Bakker (1999) and Holloway (1977). Pressure and the fugacity of H_2O in the fluid inclusion are assumed to change as diffusion proceeds, whereas the fugacity in the pore fluid is fixed by a constant temperature, pressure and composition. The concentration of a fluid component in quartz at the inclusion rim is directly related to the fugacity in the inclusion, according to the partitioning coefficient K (see Appendix A, Eq. (A9)), similarly to that of the rim of the quartz grain. At constant temperature and pressure, the partitioning coefficient between quartz and a fluid is assumed to be similar at the fluid inclusion wall and the grain boundary. However, it is likely that pressure gradients and dissimilarities in fluids cause a variation in K values between the inclusion- and grain-boundaries within the quartz.

Equilibrium and disequilibrium starting conditions for this bulk diffusion model are schematically illustrated in Fig. 4. In an initial state, the fugacity/concentration profile between fluid inclusion and quartz is equal to that for pore fluid and quartz if the fluids are similar

Table 3
Diffusion coefficients for hydrogen in β-quartz, at 800 °C and variable water pressures (obtained directly from water, without buffer).

Exp Nr.	p(H_2O) MPa	Fluid source	Exp. time s	μmol H per mol Si	D m^2 s^{-1}
N-600	1090	H_2O (// c)	$1.95 \cdot 10^5$	55 ± 10	$(3.8 \pm 2.8) \cdot 10^{-12}$
N-606	1090	H_2O (⊥ c)	$4.05 \cdot 10^5$	42 ± 10	$(1.2 \pm 0.8) \cdot 10^{-12}$
N-603	1120	H_2O (⊥ c)	$4.83 \cdot 10^5$	50 ± 10	$(1.3 \pm 1.0) \cdot 10^{-12}$
N-604	1150	H_2O (// c)	$2.31 \cdot 10^5$	45 ± 10	$(2.5 \pm 1.6) \cdot 10^{-12}$
N-602	1170	H_2O (// c)	$2.26 \cdot 10^5$	54 ± 10	$(3.1 \pm 2.4) \cdot 10^{-12}$
N-570	1530	H_2O (// c)	$1.75 \cdot 10^5$	71 ± 10	$(7.0 \pm 3.8) \cdot 10^{-12}$

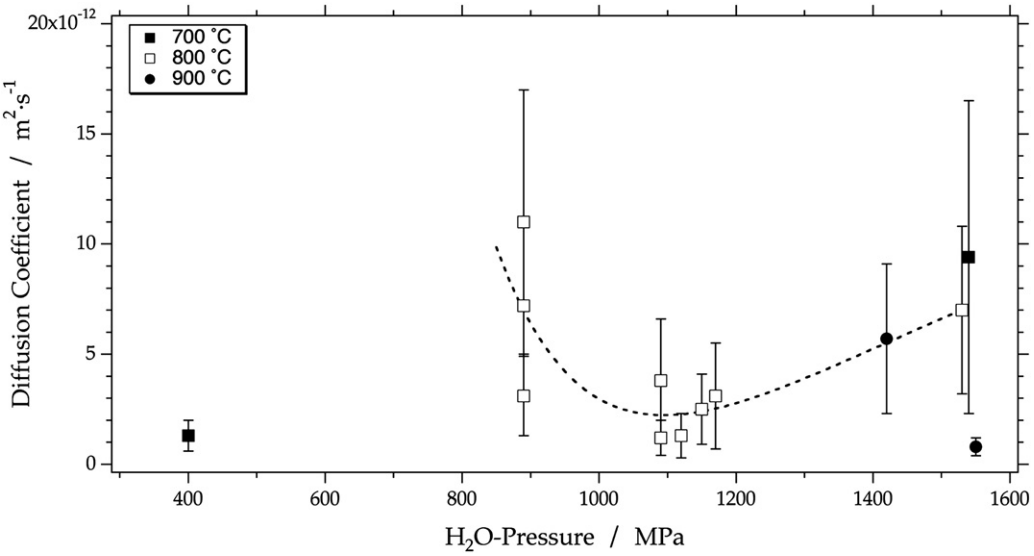

Fig. 2. Recalculated diffusion coefficients of water through quartz at variable external H_2O-pressure and temperature according to data from Kronenberg et al. (1986).

at equal temperature and pressure conditions (Fig. 4a). In this case, the quartz crystal has an equal fluid distribution and, consequently, diffusion will not take place. Fig. 4b illustrates disequilibrium conditions in the quartz directly at the pore contact, where the pore fluid has now a higher fugacity. Due to partitioning, the concentration in quartz will tend to reach a higher value in order to reach an equilibrium state with the pore fluid (Fig. 4c). As a consequence, the quartz contains a gradient in fluid concentration and the fluid component will start to flow from the pores towards the fluid inclusion. It must be noted that a variety in H_2O concentration in a quartz crystal may also represent specific equilibrium conditions, due to local variations in pressure/stress conditions. For example, high pressures in quartz adjacent to overpressurized inclusions may cause a higher (or lower) solubility of H_2O than in more distant quartz. This concentration gradient will not induce diffusion, because it reflects a pressure gradient in the quartz.

5.2. Mathematical model

The diffusion of fluid through quartz is assumed to involve two distinct types of radial non-steady state diffusion models in the present study. The diffusion of fluid from the pores into the quartz crystal is modelled according to an infinite external source (pores) at the quartz rim. In other words, the H_2O fugacity has a constant value at $r_q > b$, and the quartz has initially a uniform concentration, i.e. $c_{H_2O}^{qtz}(r,0)$ which does not necessarily represent an equilibrium solubility. It is assumed that fluid inclusions have only a minor influence in this diffusion model because of their relatively small sizes. The

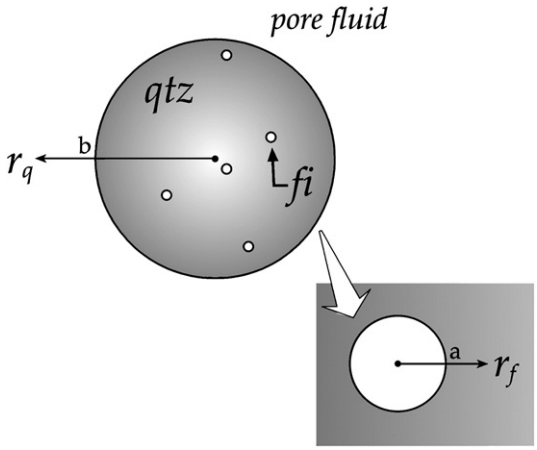

Fig. 3. Schematical model for diffusion in a spherical quartz-grain with radius b (a measure of r_q), and a fluid inclusion (fi) with radius a (a measure of r_f).

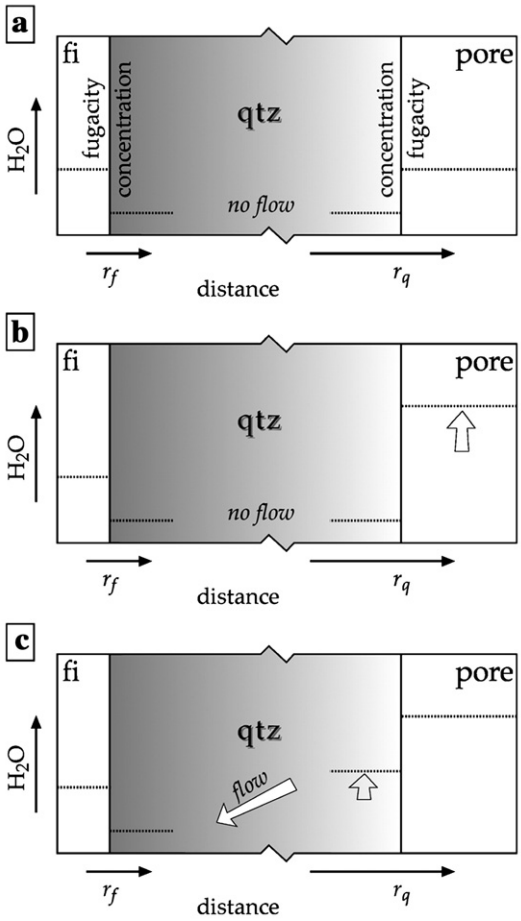

Fig. 4. Schematical illustration of H_2O concentration gradient in a quartz grain between a fluid inclusion and pore fluid with variable H_2O fugacity. See text for further details.

concentration profile in quartz can be described with Eq. (4) (see also Crank, 1979, Eq. 6.18)

$$c^{qtz}_{H_2O}\left(r_q,t\right) = (c_1 - c_0) \times\left[1 + \frac{2b}{\pi\cdot r_q}\sum_{n=1}^{\infty}\left(\frac{(-1)^n}{n}\sin\left(\frac{n\pi\cdot r_q}{b}\right)\exp\left(\frac{-n^2\pi^2 D\cdot t}{b^2}\right)\right)\right] + c_0 \quad (4a)$$

$$c_0 = c^{qtz}_{H_2O}(r,0) \quad (4b)$$

$$c_1 = c^{qtz}_{H_2O}(b,t) \quad (4c)$$

where c_1 is directly obtained from the fugacity of H_2O in the pores according to Eq. (A9). The development of a concentration profile in quartz, using Eq. (4), is illustrated in dimensionless arbitrary units for time, distance and concentration in Fig. 5. At $r_q = 0$, Eq. (4) is undefined, therefore, r_q is set to 10^{-18} m at zero distance. The summation to infinity in Eq. (4) can be shortened to a number of steps defined according to Eq. (5):

$$n_{max} = 20 + 0.3\cdot\left(\frac{D\cdot t}{b^2}\right)^{-0.7} \quad (5)$$

Initially (before $t = 0$), the concentration of the fluid in quartz is 0.10. At $t = 0$, the fugacity in the pores is abruptly changed which must eventually result in a concentration of 0.01 in the entire quartz crystal. It is assumed that the concentration in quartz directly adjacent to the pore space is in equilibrium with the pore fluid at all times (according to Eq. (A9)). The gradient in concentration in the quartz grain defines the direction of fluid flow. At $t = 500$, the concentration in the centre of the crystal has already dropped to 0.036, whereas at $t = 1000$, the concentration in the entire crystal is nearly adapted to the new equilibrium conditions.

Diffusion related to fluid inclusions is modelled according to the theory of an instantaneous point source (see also Crank, 1979, Eq. 3.8). The point source is a sphere with radius a (see Fig. 3), and represents a fluid inclusion with a certain amount of fluid components that are able

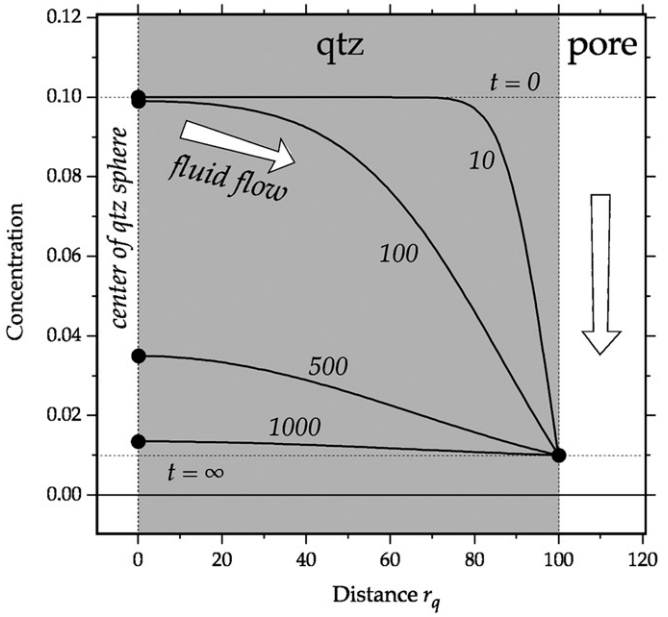

Fig. 5. Concentration profiles as a function of distance from the center in quartz according to Eq. (4). The increasing dimensionless arbitrary time unit (0, 10, 100, 500, 1000, and ∞) illustrates the development of the concentration profile from concentration c_0 (0.1) towards concentration c_1 (0.01). The dimensionless arbitrary value for the diffusion coefficient is 4.

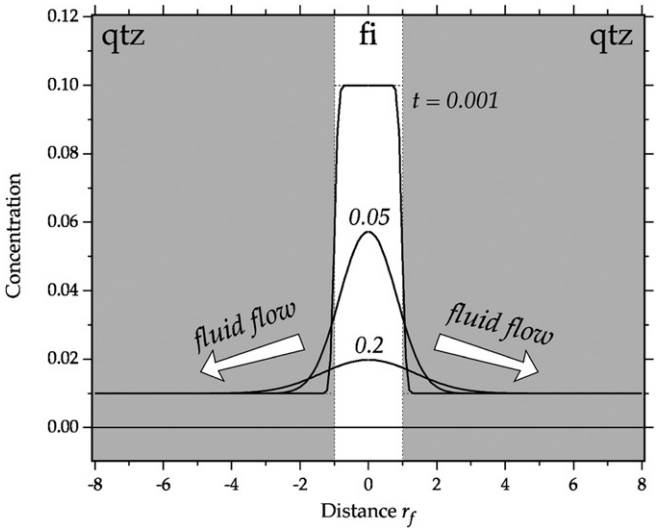

Fig. 6. Concentration profiles in quartz as a function of distance from the center of a fluid inclusion, according to Eq. (6). The same parameters as in Fig. 5 are used for the calculations.

to diffuse through the quartz. The radially concentration profile in quartz around the fluid inclusion is described with Eq. (6).

$$c^{qtz}_{H_2O}\left(r_f,t\right) = c_0 + \frac{(c_1 - c_0)}{2}\cdot\left[erf\left(\frac{a + r_f}{2\sqrt{D\cdot t}}\right) + erf\left(\frac{a - r_f}{2\sqrt{D\cdot t}}\right)\right] - \frac{(c_1 - c_0)}{r_f}\sqrt{\frac{D\cdot t}{\pi}}\cdot\left[\exp\left(\frac{-\left(a - r_f\right)^2}{4\cdot D\cdot t}\right) - \exp\left(\frac{-\left(a + r_f\right)^2}{4\cdot D\cdot t}\right)\right] \quad (6a)$$

$$c_1 = c^{qtz}_{H_2O}(a,0) \quad (6b)$$

where c_0 ("background" concentration) is defined according to Eq. (4), and c_1 is directly related to the original fugacity in the fluid inclusion, erf is the "error function". Fig. 6 illustrates the development of a concentration profile around a spherical fluid inclusion (diameter 2) using the same dimensionless arbitrary units for distance, time, diffusion coefficient and concentration as for diffusion in the quartz grain from Fig. 5. Before $t = 0$, the fugacity of H_2O in the inclusion is in equilibrium with again concentration of 0.10 in quartz. At $t = 0$ the concentration in the quartz abruptly changes to 0.01, which results in diffusion of H_2O from the inclusion in to the quartz. At $t = 0.2$, the inclusion is already nearly re-equilibrated to the new equilibrium values. Comparison of the arbitrary time values in Figs. 5 and 6 indicates that fluid inclusions are nearly instantaneously adapted to new equilibrium conditions of H_2O solubility in quartz, whereas the entire quartz grain requires about 10^5 more time to reach the same equilibrium conditions.

The concentration within a solid point source (at $r_f < a$) according to Eq. (6) is variable (see Fig. 6). However, fluid inclusions must have a uniform fugacity within a sphere of radius a. Consequently, the point-source model is only an approximation to the behaviour of fluid inclusions. The model may predict substantial differences between the concentration at $r = 0$ and $r_f = a$ (see Fig. 6). In this study, the concentration at $r = 0$ is proposed to represent the bulk fugacity within the inclusion according to Eq. (A9), and its variation with time is given by Eq. (7):

$$lim_{r\to 0}\, c^{qtz}_{H_2O}\left(r_f,t\right) = K\cdot f^{fi}_{H_2O}(t) \quad (7a)$$

$$f^{fi}_{H_2O}(t) = \frac{c_0}{K} + \left(f^{fi}_{H_2O}(0) - \frac{c_0}{K}\right)\cdot\left[erf\left(\frac{a}{2\sqrt{D\cdot t}}\right) - \frac{a}{\sqrt{\pi\cdot D\cdot t}}\exp\left(\frac{-a^2}{4\cdot D\cdot t}\right)\right] \quad (7b)$$

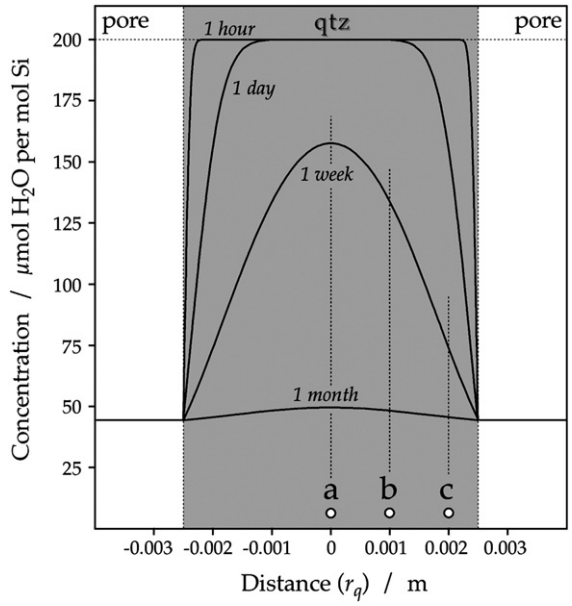

Fig. 7. Example calculation of concentration profiles in a spherical quartz grain according to Eq. (4) using $D = 10^{-12}$ m^2 s^{-1} and $k = 0.96216 \cdot 10^{-6}$ mol/Pa per mol Si. See text for further details.

where $f^{fi}_{H_2O}(0)$ is the initial fugacity within the fluid inclusion. The fugacity at the inclusion rim (at $r_f = a$) is described according to Eq. (8):

$$f^{fi}_{H_2O}(t) = \frac{c_0}{K} + \left(f^{fi}_{H_2O}(0) - \frac{c_0}{K}\right) \cdot \left[\frac{1}{2} erf\left(\frac{a}{2\sqrt{D \cdot t}}\right) - \frac{\sqrt{D \cdot t}}{a\sqrt{\pi}}\left(1 - \exp\left(\frac{-a^2}{D \cdot t}\right)\right)\right] \quad (8)$$

Alternatively, a uniform fugacity in the fluid inclusion can be approximately estimated from an average value of the concentration profile obtained from Eq. (6) between $r_f = 0$ (Eq. (7)) and $r_f = a$ (Eq. (8)). The concentration is approximately equal to the value obtained from Eq. (7) at relatively low $D \cdot t$ values (e.g. for $t = 0.001$ in Fig. 6), whereas at high $D \cdot t$ values the average concentration equals the average value of Eqs. (7) and (8).

5.3. Example calculation

To illustrate diffusive loss of H_2O from fluid inclusions according to the Eqs. (6)–(8), a theoretical example has been worked out using the previously estimated diffusion coefficients. The computer package "FLUIDS" (Bakker, 2003) includes the program "ReqDif" in order to reproduce this example and to calculate any diffusive loss or gain of fluid inclusions according to self-defined parameters. The program includes a variety of equations of state to calculate fluid fugacities in pores and inclusions of pure H_2O (Haar et al., 1984), pure CO_2 (Span and Wagner, 1996), pure CH_4 (Setzmann and Wagner, 1991), binary mixtures of H_2O–CO_2 (Holloway, 1977; Bakker, 1999), binary mixtures of H_2O–NaCl (Anderko and Pitzer, 1993), and mixtures of H_2O–CO_2–CH_4–NaCl (Duan et al., 1995, 2003). The program "ReqDif" is available on the University of Leoben web site at http://fluids.unileoben.ac.at.

Inclusions are formed in quartz crystals at 500 °C and 500 MPa (α-quartz stability field), trapping a pure H_2O fluid from the pores. The molar volume and fugacity of H_2O at these conditions are calculated at 20.56 cm$^3 \cdot$mol^{-1} and 207.9 MPa, respectively (Haar et al., 1984). We assume that the equilibrium concentration of H_2O in quartz is 200 µmol H_2O per mol Si at these conditions, consequently K equals $0.96216 \cdot 10^{-6}$ mol/Pa per mol Si (see Eq. (A9)). The diffusion coefficient is assumed to be 10^{-12} m^2 s^{-1}. Subsequently, the rock is uplifted at constant temperature to a pressure of 100 MPa, and the pore fluid remains pure H_2O. At these conditions the fugacity of H_2O in the pores decreases to 45.9 MPa and the molar volume increase to 34.11 cm^3 mol^{-1}. The H_2O fugacity in the fluid inclusions remains 207.9 MPa at these conditions. Furthermore, it is assumed that the inclusions are not able to change their total volume (e.g. by micro-cracking or decrepitation), and that K has a constant value. Consequently, the equilibrium concentration of H_2O in quartz at these conditions is 44 µmol H_2O per mole Si. The concentration profile in a spherical quartz grain (Fig. 7) illustrates that within one month the concentration of H_2O has already nearly reached an equilibrium value. This fast process implies a nearly instantaneous re-equilibration of the quartz grain at a geological time scale. Example spherical fluid inclusions are positioned in the centre, at 1 mm and 2 mm from the centre, respectively (a, b and c in Fig. 7). The inclusions are calculated to change their fugacity instantaneously, corresponding to the temporary concentration in the quartz grain. Inclusion c reaches faster re-equilibrated values than inclusion a as it is located closer to the rim. After one week (see Fig. 7) the concentrations in inclusions a, b, and c are 157, 133 and 73 µmol H_2O per mol Si, respectively. This corresponds to H_2O fugacities of 163.2, 138.2 and 75.9 MPa, respectively in fluid inclusions. The molar volume of these inclusions has changed to 21.37, 22.01 and 25.59 cm$^3 \cdot$mol^{-1}, which corresponds to internal pressures of 426, 377 and 213 MPa, respectively. Inclusion a has lost 3.8 mol% H_2O, inclusion b has lost 6.6 mol% and inclusion c has lost 19.7 mol% after one week. Finally, each inclusion will loose 39.7 mol% H_2O to reach the re-equilibration conditions. Similar results are obtained if the equilibrium concentration in quartz at 500 °C and 500 MPa is only 20 µmol H_2O per mol Si, with a K value of $0.0962 \cdot 10^{-6}$ mol/Pa per mol Si. It must be noted that the assumed values for diffusion coefficients, equilibrium solubility and K values are only approximately (see previous paragraph 3 and 4). Further experimental studies have to be performed to find reliable numbers for these parameters.

6. Discussion

6.1. Comparison to diffusion model Qin et al. (1992)

In the present study, diffusive loss or gain of H_2O from inclusions is the only process considered to change the concentration in

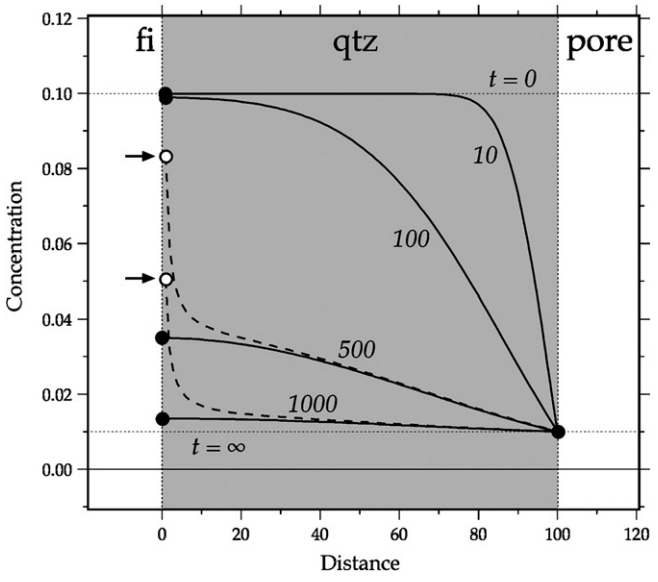

Fig. 8. Dimensionless concentration profiles in quartz around a spherical fluid inclusion in the center, according to the model of Qin et al. (1992). The same parameter values as in Fig. 5 are used. The dashed lines indicate concentration profile for an inclusion with diameter 1, the solid curves for diameter 0.1.

inclusions, similar to the model of Qin et al. (1992). Concentration profiles in quartz calculated with the model of Qin et al. (1992) and the present study are directly compared in Fig. 8, with the same dimensionless arbitrary units for distance, time, diffusion coefficient and concentration that is also used for diffusion in Fig. 5. Both models predict similar concentration profiles (solid curves in Fig. 8) after each time interval ($t=10$, 100, 500 and 1000) in a quartz crystal with relatively small fluid inclusions, i.e., with a size ratio of 10^{-3} or less (radius spherical inclusion to radius spherical quartz crystal). As previously mentioned, size ratios for natural fluid inclusions are in general in the range of 10^{-4} to 10^{-5}. Therefore, diffusion and concentration profiles in quartz are obtained by relative simpler mathematical procedures from this study (Eqs. (4)–(8)) compared to the model of Qin et al. (1992). For larger inclusions (size ratio larger than 10^{-2}) both models deviate increasingly at larger diffusion times (see dashed curves for $t=500$ and 1000 in Fig. 8). These curves indicate less alteration for extremely large inclusions according to the model of Qin et al. (1992) compared to the values obtained in this study.

The change of mass H_2O in a spherical fluid inclusion with time due to diffusion is defined according to Eq. (9) (c.f. Eq. 1 in Qin et al., 1992).

$$\frac{dQ^{fi}_{H_2O}}{dt} = \frac{4}{3}\pi a^3 \cdot \frac{\partial}{\partial t}\left(\rho^{fi} \cdot w_{H_2O}\right) \tag{9}$$

where Q is mass (in g), t is time (in s), w_i is the mass fraction, ρ^{fi} is the fluid inclusion density (in g/cm^3) and a is the radius of a spherical inclusion. The change in mole H_2O with time (i.e. flux) is expressed in Eq. (10).

$$\frac{dn^{fi}_{H_2O}}{dt} = \frac{4}{3}\pi a^3 \cdot \frac{\partial}{\partial t}\left(\frac{y_{H_2O}}{V^{fi}_m}\right) \tag{10}$$

where n is amount of substance (in mol), y is the mole fraction, and V_m is the molar volume of the fluid inclusion. These properties of fluid inclusions can be directly related to the parameters from the quartz crystal at equilibrium conditions according to Eqs. (A1) and (A9):

$$\frac{dn^{fi}_{H_2O}}{dt} = \frac{4}{3}\pi a^3 \cdot \frac{\partial}{\partial t}\left(c^{qtz}_{H_2O}\frac{H \cdot V^{qtz}_m}{10^3 \cdot \varphi_{H_2O} \cdot p \cdot V^{fi}_m}\right) \tag{11}$$

The flux of H_2O molecules in the quartz through the surface of the spherical inclusion is defined according to Fick's first law of diffusion and is directly related to the change within the fluid inclusion (Eq. (12)).

$$J = -D\frac{\partial u}{\partial r} \tag{12a}$$

$$\frac{dn}{dt} = \text{area} \cdot \text{flux} \tag{12b}$$

$$\frac{dn^{qtz}_{H_2O}}{dt} = 4\pi a^2 \cdot D\frac{\partial c^{qtz}_{H_2O}}{\partial r} \tag{12c}$$

where J is the flux, D is the diffusion constant (m s^{-1}), r is the radial distance (m), and $c_{H_2O}{}^{qtz}$ is the concentration of H_2O in quartz (mol·L^{-1}). The combination of Eqs. (11) and (12) results in:

$$\frac{\partial}{\partial t}\left(c^{qtz}_{H_2O}\frac{H \cdot V^{qtz}_m}{10^3 \cdot \varphi_{H_2O} \cdot p \cdot V^{fi}_m}\right) = 3\frac{D}{a} \cdot \frac{\partial c^{qtz}_{H_2O}}{\partial r} \tag{13}$$

The values or H, p, φ and V^{fi}_m change with time during diffusion of H_2O to or from the inclusion, and, therefore, cannot be separated from the differential in Eq. (13). Qin et al. (1992) gave simplifications of this formula (see Eq. 6 in Qin et al., 1992) by assuming these values to be independent of time, and H_2O to behave as an ideal gas in an ideal mixture with CO_2.

6.2. Re-equilibration rates of fluid inclusions

Experimental studies (e.g. Sterner and Bodnar, 1989; Bakker and Jansen, 1990) have illustrated that fluid properties of inclusions can be altered within relatively short experimental time. Consequently, it was assumed that diffusive leakage from fluid inclusions can be significant during uplift of metamorphic rock. This hypothesis was confirmed by the theoretical considerations of Qin et al. (1992), who illustrated that bulk-diffusion may affect most inclusions within several 10000 of years. For example, a 10 μm radius spherical inclusion containing a mixture of H_2O and CO_2 in a 1 mm radius quartz grain reaches half the partial H_2O pressure difference after 7930 years (see also Table 2 in Qin et al., 1992). A larger inclusion (e.g. 25 μm radius) reaches this amount of loss after 46360 years. As a consequence, it is expected that all fluid inclusion will lose significantly amounts of H_2O during exhumation of deep rock. It must be noted that this model predicts that extremely large inclusions (e.g. for $\alpha=0.9$, see Qin et al., 1992) will not suffer significant loss of H_2O, and remain useful

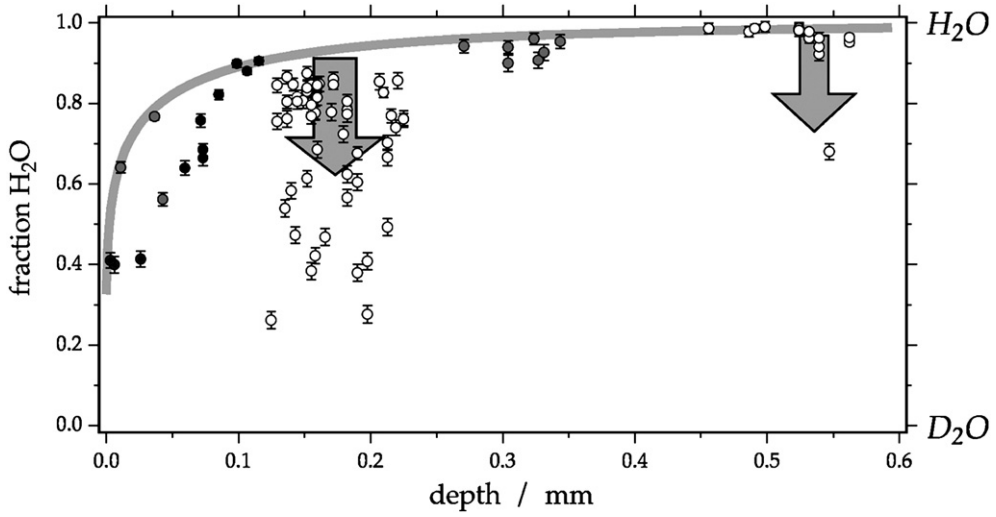

Fig. 9. Fraction of H_2O in a pseudo binary H_2O–D_2O solution in synthetic fluid inclusions as a function of depth within the quartz crystal (from Bakker, 2007).

indicators of metamorphic fluids. The diffusion coefficient selected by Qin et al. (1992), i.e. $D = 10^{-17}$ m^2 s^{-1}, corresponds to oxygen (O_2) diffusion in quartz, which has been discussed in the previous paragraph to be about 10^6 times slower than hydrogen diffusion in the form of H_2O. Re-equilibration rates are extremely effected by the selected diffusion coefficient and are reduced to several months by choosing $D = 10^{-12}$ m^2 s^{-1}.

Preliminary studies on experimental re-equilibration of fluid inclusions in quartz by Bakker and Diamond (1999, 2003) and Bakker (2007) indicate that a gradient in the chemical potential of H_2O and D_2O between inclusions and pores at constant temperature and pressure is a driving force to diffuse H_2O/D_2O through quartz, whereas CO_2 and NaCl remain immobile. Initially H_2O–CO_2-rich synthetic fluid inclusions were re-equilibrated in a D_2O pore fluid, and reveal a decrease in H_2O content in all the inclusions after experimentation: the concentrations have values between 96.2 and 25.8 mol% H_2O with respect to the H_2O–D_2O pseudobinary (Fig. 9). The extent of H_2O–D_2O exchange depends partly on the depth of the inclusions within the quartz disc, which can be directly related to bulk-diffusion (grey thick curve in Fig. 9). However, most inclusions indicate a higher content of D_2O (vertical arrows in Fig. 9), most probably due to additional migration along nano-cracks and dislocations (see also Bakker and Jansen, 1990).

These experimental studies and theoretical considerations have far reaching consequences, as also isotopic compositions of both fluids and host-mineral will rapidly change with those diffusion coefficients. The main principle of isotope geology and fluid inclusion research is violated. The conservation of the fluid content in inclusions can only be guaranteed if several of the main assumptions of these diffusion models are incorrect. First, the surface of the quartz grain is assumed to be completely in contact with a fluid phase according to the model. The porosity of metamorphic rock is extremely low (less than 1 vol.%), therefore, there is only very limited contact between one quartz grain and a pore fluid. This may reduce the effective diffusion in to quartz grains drastically. Moreover, this restriction may cause a spread in re-equilibration behaviour in an assemblage of fluid inclusions. Second, diffusion will also be limited if pore fluid and the fluid in inclusions remain similar during uplift of the rock. Third, diffusion will be highly ineffective in sedimentary and diagenetic rock because the temperature in those environments is too low (c.f. Arrhenius plot, Eq. (1)). Fourth, the estimated values of diffusion coefficients may be highly influenced by additional fluid migration paths, such as nano-cracks, stacking-faults and dislocation. Moreover, the accuracy of the estimated diffusion coefficients is extremely low, and further research is required to characterize diffusion processes in anhydrous minerals.

6.3. Textural development in underpressurized fluid inclusions

Experimental studies on re-equilibration of fluid inclusions have revealed the development of irregular shaped inclusion walls in underpressurized fluid inclusions (e.g. Pécher, 1981; Sterner and Bodnar, 1989; Bakker and Jansen, 1991). This textural development was not observed in overpressurized fluid inclusions. Similar textures have also been observed in natural fluid inclusions that are assumed to have re-equilibrated (e.g. Ayllon et al., 2003). The mechanism responsible for the formation of this texture is not well understood. Sterner and Bodnar (1989) suggested a type of exsolution of H_2O in quartz to be responsible for this texture ("implosion halos"). However, this process would result in a randomly distribution of small pure H_2O inclusions within the entire quartz grain; and it cannot explain the nearly "closure" of the parental inclusion. It is more likely that the mechanism is controlled by a variation in solubility of quartz in water. In underpressurized fluid inclusions, a pressure gradient occurs in a small zone in the quartz adjacent to the fluid inclusions (Fig. 10a, see also Fig. 4 in Bakker and Jansen, 1994). Within this zone the pressure is lower than in quartz near the grain boundary. The solubility of quartz

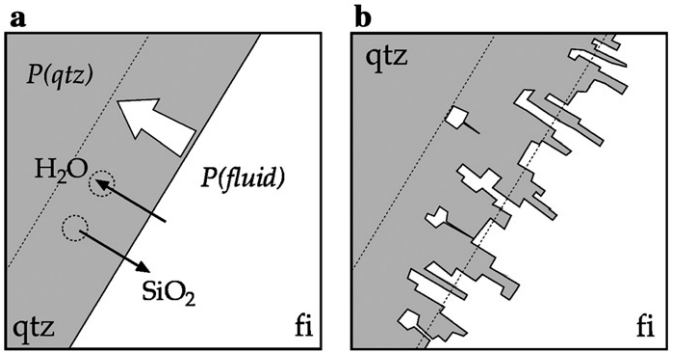

Fig. 10. Schematical illustration of the rim of a fluid inclusion with an "underpressure"; (a) the arrow indicates the pressure gradient in the quartz (from low to high); and (b) recrystallisation effect due to solubility differences of quartz in water.

in water increases at higher pressures and constant temperature (e.g. Newton and Manning, 2000). Quartz located deeper in the crystal (i.e. away from the fluid inclusion) in contact with free water will dissolve, whereas it will be precipitated at positions of lower solubility, i.e. at the fluid inclusion wall (Fig. 10b). The availability of water deeper in the quartz crystal may result from diffusion processes along numerous crystal defects and nano-cracks, which are induced by local stress. The extent of "implosion halos" around underpressurized fluid inclusions (see Fig. 8 in Sterner and Bodnar, 1989) illustrates the limits of the pressure gradient in the quartz crystal. This process does not change the bulk density and composition of fluid inclusions.

7. Summary and conclusions

Bulk diffusion of water-related species through quartz is able to change the fluid properties of inclusions. The rate of change is highly disputable because of high uncertainties in knowledge about the nature of the diffusing components, diffusion coefficients and solubility of water in quartz.

Diffusing H_2O, OH^- and H_2 molecules are the most efficient particle to transport oxygen and hydrogen through the quartz crystal. These components are extrinsic point defects, i.e. substitutional and intrinsic impurities, in the quartz host. The solubility of these components has not been sufficiently quantified in literature. Diffusion coefficients of water and oxygen have been estimated only with one-dimensional diffusion models, mainly in β-quartz. Temperature and pore fluid concentration dependencies cannot be obtained from the available data, but a $D = 10^{-12}$ m s^{-1} ($\pm 60\%$) between 700 and 900 °C is considered a plausible diffusion coefficient for water in quartz.

A three-dimensional diffusion model is proposed in this study to characterize bulk diffusion in quartz with randomly distributed fluid inclusions. Diffusion from the pore fluid into the quartz grain is modelled according to an infinite external fluid source around a spherical grain. Diffusion from fluid inclusions is modelled according to the theory of an instantaneous point source. The rate of fluid loss or gain is relatively high for inclusions of variable sizes, using the re-evaluated diffusion constants. Within a few 10,000 of years, most inclusions will completely adapt to new fluid conditions in the pore space at high temperatures and pressures. The effect of diffusion processes can be calculated with the computer program "ReqDif", that is included in the software package "FLUIDS", available at the web site http://fluids.unileoben.ac.at.

In contrast, the efficiency of this diffusion model is reduced by several important restrictions: 1. the values of diffusion coefficients are highly imprecise and cannot be appointed to one specific diffusing component, moreover, the accuracy cannot be determined; 2. the porosity in metamorphic rock is very low, therefore, a gradient between pore fluids and fluid inclusions is only present in a very small

part of the grain; 3. the temperatures in sedimentary and diagenetic environment is too low for effective diffusion; and 4. diffusion along micro-cracks and dislocations is a more efficient process to change fluid inclusions. Therefore, it is assumed that bulk diffusion plays only a minor role in re-equilibration processes of natural fluid inclusions.

Acknowledgements

I thank Tom Andersen and an anonymous reviewer for constructive comments that improved the presentation of my research.

Appendix A

The solubility of H_2O-related extrinsic impurities in quartz can be expressed in a partitioning coefficient (k) and Henry's constant (H). Both k and H are directly related according to equilibrium thermodynamics (see Prausnitz et al., 1986), and depend on temperature and pressure. The partitioning coefficient relates directly concentrations of water in the pore fluid and in the quartz (Eq. (A1)).

$$c^{qtz}_{H_2O} = k \cdot c^{pores}_{H_2O} \tag{A1}$$

where c is the concentration. For anhydrous minerals, water-related components are strongly partitioned in the coexisting fluid phase. The concentration can be expressed in terms of ppm (parts per million), which is, however, not S.I. conform (Taylor, 1995). Independent of the type of water-related species, the concentration is usually expressed in a ratio of number of H atoms per 10^6 Si atoms, i.e. a mole ratio. This can be transformed in a hydrogen concentration value with Eq. (A2) (in $mol \cdot L^{-1}$, conform SI).

$$c^{qtz}_{H} = \frac{q}{10^3 \cdot V^{qtz}_m} \text{ mole H / liter } SiO_2 \tag{A2}$$

where q is the value in "ppm" H/Si, and V^{qtz}_m is the molar volume of quartz (22.688 $cm^3 \cdot mol^{-1}$ at 25 °C and 0.1 MPa). The same q value can be transformed in a concentration of H_2O in quartz:

$$c^{qtz}_{H_2O} = \frac{\frac{1}{2} \cdot q}{10^3 \cdot V^{qtz}_m} \text{ mole } H_2O \text{ / liter } SiO_2 \tag{A3}$$

The equilibrium concentration represents a maximum solubility, i.e. saturation properties of quartz. The concentration of water in the pore fluid can be obtained from its density and composition. For example, a fluid mixture with a specific mole fraction for water (y_{H_2O}) and a bulk density of ρ^{pores} (in g cm^{-3}) has a water concentration according to Eq. (A4):

$$w_{H_2O} = \frac{y_{H_2O} \cdot M_r(H_2O)}{\sum_j x_j \cdot M_r(j)} \tag{A4a}$$

$$c^{pores}_{H_2O} = \frac{w_{H_2O} \cdot 10^3}{M_r(H_2O)} \cdot \rho^{pores} \text{ (in mol/L)} \tag{A4b}$$

where w_{H_2O} is the mass fraction of H_2O and $M_r(j)$ is the relative molecular mass of component j in the fluid mixture. Similarly, the concentration can be expressed in terms of bulk molar volume of the fluid (V^{pores}_m) (Eq. (A5)).

$$c^{pores}_{H_2O} = \frac{y_{H_2O} \cdot 10^3}{V^{pores}_m} \text{ (in mol/L)} \tag{A5}$$

Concentration expressed in e.g. ppm or molality, is a parameter that is not suitable to model non-ideal behaviour of solid and fluid solutions. The solubility of H_2O in quartz is best described according to an infinite dilution model, similar to that of low solubility of gases in a liquid (Henry's law, see Prausnitz et al., 1986). Equality of the fugacities of H_2O in quartz and the fluid phase defines equilibrium solubility conditions (Eq. (A6)).

$$f^{fluid}_{H_2O} = f^{qtz}_{H_2O} \tag{A6a}$$

where

$$f^{fluid}_{H_2O} = \varphi_{H_2O} \cdot y_{H_2O} \cdot p \tag{A6b}$$

$$f^{qtz}_{H_2O} = H \cdot x_{H_2O} \tag{A6c}$$

where φ and y are the fugacity coefficient and mole fraction of H_2O in the fluid phase, respectively, p is the fluid pressure, x is the mole fraction of H_2O in quartz. H has no precise thermodynamic significance but is similar to Henry's constant. Eq. (A6b) can be calculated according to an equation of state for fluid mixtures containing H_2O. The exact value of H is unknown, but it is in the order of 10^{-3} to 10^{-5} MPa. Pressure and temperature dependence of H can be similarly defined according to the Henry's constant (Eq. (A7)) (see also Bakker, 2003).

$$\left(\frac{\partial lnH}{\partial p}\right)_T = \frac{v^{\infty}_{H_2O}}{RT} \tag{A7a}$$

$$lnH = \sum_i \frac{a_i}{T^i} \tag{A7b}$$

where $v^{\infty}_{H_2O}$ is the partial molar volume of H_2O in quartz at infinite dilution, a_i are a series of constants ($i<5$). A combination of molar volumes of the phases in equilibrium and Eqs. (A1), (A5) and (A6) results in the definition of k:

$$k = \frac{\left(\varphi_{H_2O} \cdot p \cdot V_m\right)^{fluid}}{(H \cdot V_m)^{qtz}} \tag{A8}$$

where and V^{qtz}_m and V^{fluid}_m are the molar volumes (in $cm^3 \cdot mol^{-1}$) of quartz and the fluid phase. Alternatively, the concentration of H_2O in quartz can be directly related to the fugacity in the fluid phase according to Eq. (A9).

$$c^{qtz}_{H_2O} = K \cdot f^{fluid}_{H_2O} \tag{A9a}$$

$$K = \frac{10^3}{H \cdot V^{qtz}_m} \tag{A9b}$$

where K is similar to the partitioning coefficient k. The solubility in quartz can be expressed as a concentration value (mole L^{-1}), whereas the behaviour of water in the fluid must be expressed in terms of fugacity due to non-ideality of fluid mixtures. Modifications of equilibrium solubilities according to changes in fluid composition, temperature and pressure are best understood according to Eqs. (A6)–(A9).

Appendix B

The assumptions of the diffusion model according to Qin et al. (1992) were mainly applied to melt inclusions, as concentrations were expressed in "ppm's" and decoupled from inclusion density, which was assumed to remain constant. Their "ppm" values were used as a synonym for mass fractions. The complexity of their mathematical solution is caused by the chosen boundary conditions. The Laplace transformation of Fick's second law of radial diffusion (Eq. (A10)) is

often needed to find a mathematical solution for concentration profiles in quartz with relatively complex boundary conditions.

$$p\overline{c}(r,p) - c(r,0) = D\left[\frac{2}{r}\frac{\partial \overline{c}(r,p)}{\partial r} + \frac{\partial^2 \overline{c}(r,p)}{\partial r^2}\right] \quad \text{(A10)}$$

where $\overline{c}$ is the Laplace transformed concentration function (see Eq. (A11)), c is the concentration as a function of radial distance (r) and time (t), and $c(r,0)$ is the concentration at radius r and time 0.

$$\overline{c}(r,p) = \int_0^\infty \exp(-p\cdot t)\cdot c(r,t)dt \quad \text{(A11)}$$

where p is a new variable that replaces time. General solutions of Eq. (A10) are given in Eq. (A12).

$$\overline{c}(r,p) = \frac{1}{r}[A\cdot\exp(r\sqrt{p}) + B\cdot\exp(-r\sqrt{p})] + \frac{c(r,0)}{p} \quad \text{(A12a)}$$

$$\overline{c}(r,p) = \frac{1}{r}[A\cdot\sinh(r\sqrt{p}) + B\cdot\cosh(r\sqrt{p})] + \frac{c(r,0)}{p} \quad \text{(A12b)}$$

where A and B are unknown parameters that were solved by Qin et al. (1992) from their selected boundary conditions. The most important boundary condition defined by Qin et al. (1992) originates in the flux of components through the inclusion walls and the coupled change in concentration in the inclusion.

References

Aines, R.D., Kirby, S.H., Rossman, G.R., 1984. Hydrogen speciation in synthetic quartz. Physics and Chemistry of Minerals 11, 204–212.

Anderko, A., Pitzer, K.S., 1993. Equation-of-state representation of phase equilibria and volumetric properties of the system NaCl–H_2O above 573 K. Geochimica et Cosmochimica Acta 57, 1657–1680.

Angell, C.A., Shuppert, J., Tucker, J.C., 1973. Anomalous properties of supercooled water, heat capacity, expansivity, and proton magnetic resonance chemical shift from 0 to −38 °C. Journal of Physical Chemistry 77, 3092-2099.

Ayllon, F., Bakker, R.J., Warr, L.N., 2003. Re-equilibration of fluid inclusions in diagenetic-anchizonal rocks of the Cinera–Matallana coal basin (NW Spain). Geofluids 3, 49–68.

Bachheimer, J.P., 2000. Comparative NIR and IR examination of natural, synthetic, and irradiated synthetic quartz. European Journal of Mineralogy. 12, 975–986.

Bakker, R.J., 1999. Optimal interpretation of microthermometrical data from fluid inclusions: thermodynamic modelling and computer programming. Habilitation. University Heidelberg. 50 pp.

Bakker, R.J., 2003. Package FLUIDS 1. Computer programs for the analysis of fluid inclusion data and for modelling bulk fluid properties. Chemical Geology 194, 3–23.

Bakker, R.J., 2004. Raman spectra of fluid and crystal mixtures in the systems H_2O, H_2O–NaCl and H_2O–$MgCl_2$ at low temperatures: applications to fluid-inclusion research. Canadian Mineralogist 42, 1283–1314.

Bakker, R.J., 2007. Diffusion of fluids through quartz. Geochimica et Cosmochimica Acta 71, A54.

Bakker, R.J., Diamond, L.W., 1999. Reequilibration of synthetic CO_2–H_2O fluid inclusions in quartz: isofugacity experiments. Terra Nostra 99, 20–21.

Bakker, R.J., Diamond, L.W., 2003. Fluid inclusion re-equilibration experiments in quartz: chemical potential gradients. Acta Mineralogica-Petrographica, Abstracts Series 2, 95–96.

Bakker, R.J., Jansen, J.B.H., 1990. Preferential water leakage from fluid inclusions by means of mobile dislocations. Nature 345, 58–60.

Bakker, R.J., Jansen, J.B.H., 1991. Experimental post-entrapment water loss from synthetic CO_2–H_2O inclusions in natural quartz. Geochimica et Cosmochimica Acta 55, 2215–2230.

Bakker, R.J., Jansen, J.H.B., 1994. A mechanism for preferential H_2O leakage from fluid inclusions in quartz, based on TEM observations. Contributions to Mineralogy and Petrology 116, 7–20.

Brady, J.B., 1995. In: Ahrens, T.J. (Ed.), Diffusion data for silicate minerals, glasses, and liquids. AGU Reference Shelf, vol. 2, pp. 269–290.

Carslaw, H.S., Jaeger, J.C., 1986. Conduction of heat in solids, 2nd edition. Oxford University Press. 510 pp.

Catlow, C.R.A., Baram, P.S., Parker, S.C., Purton, J., Knight, K.V., 1995. Protons in oxides. Philosophical Transactions of the Royal Society of London 350, 265–276.

Cordier, P., Boulogne, B., Doukhan, J.C., 1988. Water precipitation and diffusion in wet quartz and wet berlinite, $AlPO_4$. Bulletin de Mineralogy 111, 113–137.

Crank, J., 1979. The mathematics of diffusion, 2nd edition. Oxford University Press. 414 pp.

Demouchy, S., Deloule, E., Frost, D.J., Keppler, H., 2005. Pressure and temperature-dependence of water solubility in Fe-free wadsleyite. American Mineralogist 90 (7), 1084–1091.

Dennis, P.F., 1984. Oxygen self-diffusion in quartz under hydrothermal conditions. Journal of Geophysical Research 89 (B6), 4047–4057.

Doukhan, J.C., Paterson, M.S., 1986. Solubility of water in quartz: a revision. Bulletin de Mineralogie 109 (3), 193–198.

Duan, Z., Møller, N., Weare, J.H., 1995. Equation of state for the NaCl–H_2O–CO_2 system: prediction of phase equilibria and volumetric properties. Geochimica et Cosmochimica Acta 59, 2869–2882.

Duan, Z., Møller, N., Weare, J.H., 2003. Equation of state for the NaCl–H_2O–CH_4 system and the NaCl–H_2O–CO_2–CH_4 system: phase equilibria and volumetric properties above 573 K. Geochimica et Cosmochimica Acta 67, 671–680.

Elphick, S.C., Dennis, P.F., Graham, C.M., 1986. An experimental study of the diffusion of oxygen in quartz and albite using an overgrowth technique. Contributions to Mineralogy and Petrology 92 (3), 322–330.

Farver, J.R., Yund, R.A., 1991. Oxygen diffusion in quartz: dependence on temperature and water fugacity. Chemical Geology 90, 55–70.

Freer, R., Dennis, P.F., 1982. Oxygen diffusion studies: I. A preliminary ion microprobe investigation of oxygen diffusion in some rock-forming minerals. Mineralogical Magazine 45, 179–192.

Gerretsen, J., Paterson, M.S., McLaren, A.C., 1989. The uptake and solubility of water in quartz at elevated pressure and temperature. Physics and Chemistry of Minerals 16, 334–342.

Giletti, B.J., 1986. Diffusion effects on oxygen isotope temperatures of slowly cooled igneous and metamorphic rocks. Earth and Planetary Science Letters 77, 218–228.

Giletti, B.J., Yund, R.A., 1984. Oxygen diffusion in quartz. Journal of Geophysical Research 89 (B6), 4039–4046.

Giletti, B.J., Semet, M.P., Yund, R.A., 1978. Studies in diffusion; III. Oxygen and feldspars, an ion microprobe determination. Geochimica et Cosmochimica Acta 42, 45–57.

Griggs, D., 1967. Hydrolytic weakening of quartz and other silicates. Geophysical Journal of the Royal Astronomical Society 14, 19–31.

Griggs, D., 1974. A model of hydrolytic weakening in quartz. Journal of Geophysical Research 79, 1653–1661.

Griggs, D., Blacic, J.D., 1965. Quartz: anomalous weakness of synthetic crystals. Science 147, 292–295.

Haar, L., Gallagher, J.S., Kell, G.S., 1984. NBS/NRC Steam Tables.

Haul, R., Dümbgen, G., 1962. Untersuchung der Sauerstoffbeweglichkeit in Titandioxid, Quarz und Quarzglas mit Hilfe des heterogenen Isotopenaustausches. Zeitschrift für Elektrochemie 66, 636–641.

Heggie, M., 1992. A molecular water pump in quartz dislocations. Nature 355, 337–339.

Holloway, J.R., 1977. Fugacity and activity of molecular species in supercritical fluids. In: Fraser, D.G. (Ed.), Thermodynamics in Geology, pp. 161–181.

Ingrin, J., Blanchard, M., 2006. Diffusion of hydrogen in minerals. In: Keppler, H., Smyth, R. (Eds.), Water in nominally anhydrous minerals. Reviews in Mineralogy, vol. 62, pp. 291–320.

Johnson, E.A., 2006. Water in nominally anhydrous crustal minerals: speciation, concentration, and geologic significance. In: Keppler, H., Smyth, R. (Eds.), Water in nominally anhydrous minerals. Reviews in Mineralogy, vol. 62, pp. 117–154.

Kronenberg, A.K., 1994. Hydrogen speciation and chemical weakening of quartz. Reviews in Mineralogy, vol. 29, pp. 123–176.

Kronenberg, A.K., Kirby, S.H., Aines, R.D., Rossman, G.R., 1986. Solubility and diffusional uptake of hydrogen in quartz at high water pressures; implications for hydrolytic weakening. Journal of Geophysical Research 91 (B12), 12723–12741.

Libowitzky, E., Rossman, G.R., 1997. An IR absorption calibration for water in minerals. American Mineralogist 82, 1111–1115.

Mavrogenes, J.A., Bodnar, R.J., 1994. Hydrogen movement into and out of fluid inclusions in quartz — experimental evidence and geological implications. Geochimica et Cosmochimica Acta 58, 141–148.

McLaren, A.C., Cool, R.F., Hyde, S.T., Tobin, R.C., 1983. The mechanism of the formation and growth of water bubbles and associated dislocation loops in synthetic quartz. Physics and Chemistry of Minerals 9, 79–94.

Newton, R.C., Manning, C.E., 2000. Quartz solubility in H_2O–NaCl and H_2O–CO_2 solutions at deep crustal-upper mantle pressures and temperatures: 2–15 kbar and 500–900 °C. Geochimica et Cosmochimica Acta 64, 2993–3005.

Paterson, M.S., 1982. The determination of hydroxyl by infrared absorption in quartz, silicate glasses and similar materials. Bulletin de Mineralogie 105, 20–29.

Paterson, M.S., 1986. The thermodynamics of water in quartz. Physics and Chemistry of Minerals 13, 245–255.

Pécher, A., 1981. Experimental decrepitation and re-equilibration of fluid inclusions in synthetic quartz. Tectonophysics 78, 567–583.

Prausnitz, J.M., Lichtenthaler, R.N., de Azevedo, E.G., 1986. Molecular thermodynamics of fluid-phase equilibria. Prentice Hall Inc. 600 pp.

Qin, Z., Lu, F., Anderson Jr., A.T., 1992. Diffusive reequilibration of melt and fluid inclusions. American Mineralogist 77, 565–576.

Rosa, A.L., El Barbary, A.A., Heggie, M.I., Briddon, P.R., 2005. Structural and thermodynamic properties of water related defects in alpha-quartz. Physics and Chemistry of Minerals 32, 323–331.

Setzmann, U., Wagner, W., 1991. A new equation of state and tables of thermodynamic properties of methane covering the range from the melting line to 625 K at pressures up to 1000 MPa. Journal of Physical Chemistry Reference Data 20, 1061–1155.

Sharp, Z.D., Giletti, B.J., Yoder Jr., H.S., 1991. Oxygen diffusion rates in quartz exchanged with CO_2. Earth and Planetary Science Letters 107, 339–348.

Shepherd, T.J., Rankin, A.H., Alderton, D.H.M., 1985. A practical guide to fluid inclusion studies. Blackie & Son, Glasgow. 239 pp.

Span, R., Wagner, W., 1996. A new equation of state for carbon dioxide covering the fluid region from the triple point temperature to 1100 K at pressures up to 800 MPa. Journal of Physical Chemistry Reference Data 25, 1509–1596.
Sterner, S.M., Bodnar, R.J., 1989. Synthetic fluid inclusions: VII. Re-equilibration of fluid inclusions in quartz during laboratory simulated metamorphic burial and uplift. Journal of Metamorphic Geology 7, 243–260.
Stolper, E., 1982. Water in silicate glasses: an infrared spectroscopic study. Contributions to Mineralogy and Petrology 81, 1–17.
Taylor, B.N., 1995. Guide for the use of the International System of units (SI). NIST Special Publication, vol. 811. 74 pp.
Touret, J.L.R., 2001. Fluids in metamorphic rocks. Lithos 55, 1–25.